BOUND-FREE PAIR PRODUCTION MECHANISM IN Pb–p COLLISIONS AT THE LHC*

Melek Yilmaz Şengül

Haliç University, Engineering Faculty, Electrical and Electronics Engineering
34060, İstanbul, Turkey
melekyilmazsengul@halic.edu.tr
melekaurora@yahoo.com

Received 15 September 2022, accepted 18 May 2023,
published online 14 June 2023

In this work, cross-section calculations of bound-free pair production (BFPP) are done for the mechanism in Pb–p collisions at the LHC. The BFPP cross section for the asymmetric collisions of Pb–p at the center-of-mass energies of $\sqrt{s_{NN}} = 5.02$ TeV and $\sqrt{s_{NN}} = 8.16$ TeV is computed. In order to reach the exact results, Monte Carlo integration techniques are utilized to calculate the lowest-order Feynman diagrams amplitudes via the lowest-order perturbation theory. Moreover, in this work, our cross-section results for the BFPP mechanism in Pb–p collisions at the LHC are compared with BFPP cross-section results obtained in the literature, which are reached for Pb–p collisions by using a simple scaling applied to scale the BFPP cross-section results in Pb–Pb collisions at the LHC.

DOI:10.5506/APhysPolB.54.4-A4

1. Introduction

The main construction aim of the Large Hadron Collider (LHC) is to examine the Quark–Gluon Plasma (QGP) that is only created at high temperatures and densities by the collisions of fully striped lead ($^{208}\mathrm{Pb}^{82+}$) ions. At the LHC, heavy-ion collisions are the most important case, while the other essential part of the LHC is the proton–proton collisions to discover the Higgs boson. To search for the features of QGP, the results of proton–Pb and deuteron–Pb collisions are preferred [1–3].

In the initial design of the LHC, p–Pb collisions were not planned, p–Pb collisions have been tried at the LHC up to the years 2011/2012 and successfully obtained [4]. The p–Pb experiments that were done at the LHC in 2016 are the most successful ones. These experiments were done for two different beam energies and inverted beam directions. The key parameter of

* Funded by SCOAP^3 under Creative Commons License, CC-BY 4.0.

nucleon–nucleon collisions is the center-of-mass energy of $\sqrt{s_{NN}}$. The first part of the p–Pb experiments was carried out in 2016 at the center-of-mass energy of $\sqrt{s_{NN}} = 5.02$ TeV. The second part of these experiments was done also at the center-of-mass energy of $\sqrt{s_{NN}} = 8.16$ TeV [1].

During Run 2 (2015–2018), the LHC worked approximately with two times higher energy and achieved Pb–Pb collisions with an order of magnitude higher luminosity compared to Run 1. As a result, the power via BFPP process increased almost by a factor of 20 in comparison with the power of the secondary beams emitted from the interaction points [5]. In this way, the importance of BFPP cross-section calculations has increased for the Pb–p collisions. For this reason, we concentrate on the asymmetric collisions of Pb–p with accelerating and colliding protons with Pb which were examined for the first time at the LHC [4, 6, 7].

The upgrade of the LHC is the High-Luminosity Large Hadron Collider (HL-LHC) to accomplish much more integrated luminosities soon. In 2028, the performance of the HL-LHC p–Pb will mostly be obtained in LHC Run 3. The p–Pb experiments and calculations will be complementary to the Pb–Pb results [1]. One of the most important impressions in heavy-ion collider physics is the bound-free pair production to the total cross section and the effects of photonuclear processes. At high energies, these processes highly contribute to the total cross section in symmetric collisions of heavy ions of high charge such as Pb–Pb collisions. However, the contribution of asymmetric collisions, such as p–Pb collisions cannot be ignored [1]. Before the experiments are done, obtaining the confidential cross-section calculation results is very important. In this work, for the first time, p–Pb cross-section calculations are done by the previously tested and the working method.

2. Formalism

In this paper, the cross section of BFPP in the asymmetric Pb–p collision as depicted in Fig. 1 is computed. The Monte Carlo method and the semiclassical approximation by utilizing the lowest-order perturbation theory in the framework of QED is used to obtain the exact results. Monte Carlo techniques were utilized in the computations of BFPP cross section, and to ensure sufficient convergence of our theoretical results, the integrands were tested at 10 M randomly chosen "positions". In the computations, the total numerical error is found to be less than 5% [8].

The number of events that creates the quark–gluon plasma depends on the inelastic hadronic cross section in heavy-ion collisions. The collision is defined as ultra-peripheral if the impact parameter b in collisions performs $b > 2R$, where R is the nuclear electric radius [1]. In heavy-ion collisions with the ion colliding peripherally, the strongly Lorentz-contracted electro-

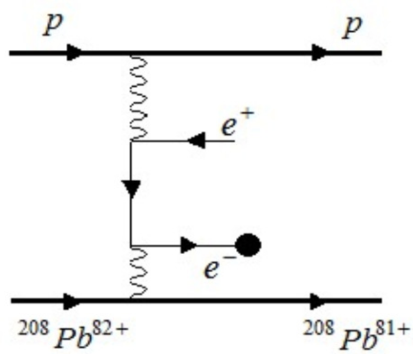

Fig. 1. Lowest-order Feynman diagram (direct diagram) for bound-free electron–positron pair production in the asymmetric Pb–p collision [8].

magnetic fields create a virtual photon flux. In ultra-peripheral collisions, the photon flux causes to occur the lepton pair production probability. This effect is not so important in p–p collisions at the LHC, but it is very important in the collisions of ions with an atomic number $Z \gg 1$. One of the colliding ions may catch a small part of the created electrons and it is finalized in a bound state. This situation is defined as BFPP and leads to a change in the ion charge. At photon energies, this process may even come true a bit smaller than $\hbar\omega = 2m_e$ as the required energy is decreased by the bound state, where $h = 2\pi\hbar$ is Planck's constant, ω is the photon angular frequency, and m_e is the electron mass [1, 9, 10].

The first-order BFPP process for the symmetric Pb–Pb collisions can be written as

$$^{208}\mathrm{Pb}^{82+} + \,^{208}\mathrm{Pb}^{82+} \to \,^{208}\mathrm{Pb}^{82+} + \,^{208}\mathrm{Pb}^{81+} + e^{+}\,. \tag{1}$$

The asymmetric BFPP for the Pb–p collision type is

$$^{208}\mathrm{Pb}^{82+} + p \to \,^{208}\mathrm{Pb}^{81+} + p + e^{+}\,. \tag{2}$$

For Pb–p collisions, the BFPP cross-section results are orders of magnitude smaller than for the symmetric Pb–Pb collisions, since the proton generates $1/82^2$ times smaller photon flux when it is compared with a lead ion [9, 11, 12].

In BFPP cross-section calculations of the asymmetric Pb–p collision, the crossed and direct terms are described by the Feynman diagrams in the lowest-order QED. In this process, the Sommerfeld–Maue wave function represents the free positron ($\Psi_q^{(+)}$) and the Darwin wave function represents the captured electron ($\Psi^{(-)}(\vec{r})$). The explicit forms of the wave functions can be found in detail in [8]. By using these wave functions, the BFPP cross section of the asymmetric Pb–p collision for the second-order perturbation theory can be written as

$$\sigma_{\mathrm{BFPP}} = \int \mathrm{d}^2 b \sum_{q<0} \left| \left\langle \Psi^{(-)} \left| S \right| \Psi_q^{(+)} \right\rangle \right|^2 = \frac{|N_+|^2}{4\beta^2} \frac{1}{\pi} \left(\frac{Z}{a_H} \right)^3 \sum_{\sigma_q} \int \frac{\mathrm{d}^3 q \, \mathrm{d}^2 p_\perp}{(2\pi)^5} \times \left(\mathcal{D}^{(+)}(q : \boldsymbol{p}_\perp) + \mathcal{D}^{(-)}(q : \boldsymbol{q}_\perp - \boldsymbol{p}_\perp) \right)^2 , \tag{3}$$

with

$$\mathcal{D}^{(+)}(q : \boldsymbol{p}_\perp) = H(-\boldsymbol{p}_\perp : \omega_{\mathrm{pr}}) \, H(\boldsymbol{p}_\perp - \boldsymbol{q}_\perp : \omega_{\mathrm{Pb}}) \, \mathcal{T}_q(\boldsymbol{p}_\perp : +\beta) , \tag{4}$$

and

$$\mathcal{D}^{(-)}(q : \boldsymbol{q}_\perp - \boldsymbol{p}_\perp) = H(\boldsymbol{p}_\perp - \boldsymbol{q}_\perp : \omega_{\mathrm{Pb}}) \, H(-\boldsymbol{p}_\perp : \omega_{\mathrm{pr}}) \times \mathcal{T}_q(\boldsymbol{q}_\perp - \boldsymbol{p}_\perp : -\beta) . \tag{5}$$

The explicit form of the scalar fields associated with proton “pr” and ion “Pb” can be expressed in momentum space as a function of the corresponding frequencies as

$$H(-\boldsymbol{p}_\perp : \omega_{\mathrm{pr}}) = \frac{4\pi Z e}{\left(\frac{Z^2}{a_H^2} + \frac{\omega_{\mathrm{pr}}^2}{\gamma^2 \beta^2} + \boldsymbol{p}_\perp^2 \right)} , \tag{6}$$

where ω_{pr} is the frequency for the proton,

$$H(\boldsymbol{p}_\perp - \boldsymbol{q}_\perp : \omega_{\mathrm{Pb}}) = \frac{4\pi Z e \gamma^2 \beta^2}{\left(\omega_{\mathrm{Pb}}^2 + \gamma^2 \beta^2 (\boldsymbol{p}_\perp - \boldsymbol{q}_\perp)^2 \right)} , \tag{7}$$

where ω_{Pb} is the frequency for the lead. The transition amplitude for both “pr” and “Pb” can be expressed as follows:

$$\mathcal{T}_q(\boldsymbol{p}_\perp : +\beta) = \sum_s \sum_{\sigma_p} \frac{1}{\left(E_p^{(s)} - \left(\frac{E^{(-)} + E_q^{(+)}}{2} \right) - \beta \frac{q_z}{2} \right)} \left[1 + \frac{\boldsymbol{\alpha} \cdot \boldsymbol{p}}{2m} \right] \times \langle \boldsymbol{u} \left| (1 - \beta \alpha_z) \right| \boldsymbol{u}_{\sigma_p}^{(s)} \rangle \langle \boldsymbol{u}_{\sigma_p}^{(s)} \left| (1 + \beta \alpha_z) \right| \boldsymbol{u}_{\sigma_q}^{(+)} \rangle . \tag{8}$$

This term represents the relationship between the intermediate photon lines and the outgoing electron–positron lines. Transition amplitude depends explicitly on the velocity of the ions (β), transverse momentum of the intermediate state ($\boldsymbol{p}_\perp$), parallel momentum of the intermediate state (p_z), and momentum of the positron (q). In this expression, $\boldsymbol{u}_{\sigma_p}^{(s)}$ is the spinor part of the intermediate state [8].

We found the expression that represents the BFPP cross section in terms of impact parameter as given below

$$\frac{\mathrm{d}\sigma_{\mathrm{BFPP}}}{\mathrm{d}b} = \int_0^\infty \mathrm{d}q\, qbJ_0(qb)\mathcal{F}(q)\,. \tag{9}$$

In this equation, there is a highly oscillatory Bessel function of the order of zero and the function $\mathcal{F}(q)$ is a six-dimensional integral which can be written as

$$\begin{aligned}\mathcal{F}(q) \;=\; & \frac{\pi}{8\beta^2}\left|N_+\right|^2\frac{1}{\pi}\left(\frac{Z}{a_H}\right)^3\sum_{\sigma_q}\int_0^{2\pi}\mathrm{d}\phi_q\int\frac{\mathrm{d}q_z\mathrm{d}^2K\mathrm{d}^2Q}{(2\pi)^7} \\ & \times\left\{H\left[\frac{1}{2}(\boldsymbol{Q}-\boldsymbol{q});\omega_{\mathrm{pr}}\right]H\left[-\boldsymbol{K};\omega_{\mathrm{Pb}}\right]\mathcal{T}_q\left[-\frac{1}{2}(\boldsymbol{Q}-\boldsymbol{q});\beta\right]\right. \\ & \left.+H\left[\frac{1}{2}(\boldsymbol{Q}-\boldsymbol{q});\omega_{\mathrm{pr}}\right]H\left[-\boldsymbol{K};\omega_{\mathrm{Pb}}\right]\mathcal{T}_q\left[\boldsymbol{K};-\beta\right]\right\} \\ & \times\left\{H\left[\frac{1}{2}(\boldsymbol{Q}+\boldsymbol{q});\omega_{\mathrm{pr}}\right]H\left[-\boldsymbol{K};\omega_{\mathrm{Pb}}\right]\mathcal{T}_q\left[-\frac{1}{2}(\boldsymbol{Q}+\boldsymbol{q});\beta\right]\right. \\ & \left.+H\left[\frac{1}{2}(\boldsymbol{Q}+\boldsymbol{q});\omega_{\mathrm{pr}}\right]H\left[-\boldsymbol{K};\omega_{\mathrm{Pb}}\right]\mathcal{T}_q\left[\boldsymbol{K};-\beta\right]\right\}\,. \end{aligned} \tag{10}$$

In Eq. (10), Z/a_H is a term coming from the electron wave function; N_+ is the normalization constant coming from the positron wave function. Here, $\boldsymbol{Q}$ and $\boldsymbol{K}$ are the new variables being the functions of $\boldsymbol{p}$ and $\boldsymbol{q}$. If Eq. (10) is numerically integrated, the following simple $\mathcal{F}(q)$ expression is obtained for a fixed value of q:

$$\mathcal{F}(q) = \mathcal{F}(0)\,\mathrm{e}^{-aq} = \sigma_{\mathrm{BFPP}}\,\mathrm{e}^{-aq}\,. \tag{11}$$

In Eq. (11), $\mathcal{F}(0)$ is equal to the total cross section of BFPP for Pb–p collisions and calculated at $q = 0$. The slope of $\mathcal{F}(q)$ is not dependent on the energies and charges of the heavy ions and it is equal to the constant value $a = 1.35\lambda_{\mathrm{C}}$ in terms of the reduced Compton wavelength of the electron ($\lambda_{\mathrm{C}} = \hbar/mc$) [13]. The probability for BFPP in terms of impact parameter can be given as

$$P_{\mathrm{BFPP}}(b) = \frac{1}{2\pi b}\frac{\mathrm{d}\,\sigma_{\mathrm{BFPP}}}{\mathrm{d}b} = \sigma_{\mathrm{BFPP}}\frac{a}{2\pi\left(a^2+b^2\right)^{3/2}}\,, \tag{12}$$

and the cross section can be written as

$$\sigma_{\mathrm{BFPP}} = \int_0^\infty P_{\mathrm{BFPP}}(b)\,\mathrm{d}^2b = \int_0^\infty P_{\mathrm{BFPP}}(b)2\pi\,b\,\mathrm{d}b\,. \tag{13}$$

Detailed information on the BFPP cross-section calculations can be found in our previous papers [14–17].

3. Results and discussions

At energies of $\sqrt{s_{NN}} = 5.02$ TeV and $\sqrt{s_{NN}} = 8.16$ TeV, cross-section results of BFPP in p–Pb collisions are first published in [1]. In the experiments at ALICE, the beam direction is reversed to fill a wider rapidity range, *i.e.*, the proton beams which are initially put in Beam 1 (p–Pb) are directed into Beam 2 (Pb–p) and Pb beams are directed from Beam 2 into Beam 1. In the cross-section analysis, the total cross section which depends on the beam direction slightly changes. The p–Pb configuration gives a slightly larger value for cross section than the value obtained in [1]. In this work, our BFPP cross-section results for Pb–p collisions are compared with the cross-section results that are given in [1] as a table.

Authors did their BFPP cross-section calculations for the p–Pb system configuration and energy by using a simple scaling that is applied to scale BFPP cross-section results in Pb–Pb collisions at the LHC. In [1], both the EMD (Electromagnetic Dissociation) and BFPP cross sections were calculated. The BFPP into the $1s$ bound state behaves as explained in [9, 11, 12],

$$\sigma_{1s} = Z_1^5 Z_2^2 a \log(\gamma_c/\gamma_0)\,. \tag{14}$$

In this equation, index 1 refers to the ion that captures the electron and index 2 refers to the projectile ion. γ_0 and a values can be obtained in [11]. The γ_c is the fixed-target Lorentz factor.

The EMDm cross section is expected to scale approximately like the BFPP cross section (where number m represents the produced electron–positron pairs) [18, 19]

$$\sigma_{\mathrm{EMDm}} \propto Z_2^2 \log(\gamma_c)\,. \tag{15}$$

According to the total scaling behaviour of $\sigma_{\mathrm{BFPP/EMD}} \propto Z_2^2 \log(\gamma_c)$ (see Eqs. (14) and (15)), the scaling factors are calculated for the fixed-target Lorentz factors. This scaling is implemented to the different EMDm and BFPPm cross sections in Pb–Pb collisions. These BFPP cross-section results in Pb–p collisions at the LHC that are reached in [1] with the center-of-mass energy $\sqrt{s_{NN}} = 5.02$ TeV and the center-of-mass energy $\sqrt{s_{NN}} = 8.16$ TeV at the LHC are equal to 41.3 mbarn and 43.7 mbarn, respectively. The simple scaling method that is explained above is used to calculate Pb–p collisions cross-section results. It is not a well-known and not verified method. It is a kind of approximation to predict the experiment results. For these reasons, there is a need for more accurate calculations for the given parameters. In contradistinction to [1], our method was tested many times before for symmetric A–A collisions for BFPP calculations and worked well. Also, we applied our method for asymmetric BFPP cross-section calculations, used previously to calculate BFPP cross sections for p–Bi and p–Au collisions at the NICA collider and we reached satisfactory results [14].

The BFPP cross-section results in Pb–p collisions with the center-of-mass energy $\sqrt{s_{NN}} = 5.02$ TeV and the center-of-mass energy $\sqrt{s_{NN}} = 8.16$ TeV at the LHC are equal to 31.97 mbarn and 34.43 mbarn in our work, respectively. When we compare our BFPP cross-section results for Pb–p collisions with the LHC results that were reached in [1], it is seen that our cross-section results are approximately 20% lower than the results given in [1]. The method used in [1] is a rough estimation method to have an idea about the future experiment results. It gives the approximate results, however, our method is more precise and two results differ from each other by 20%. Consequently, we have obtained acceptable values by means of the Monte Carlo method used in [14], as we have expected.

4. Conclusions

In the present work, the BFPP cross-section calculations of Pb–p collisions at the LHC are presented. The BFPP cross-section results for Pb–p collisions with the center-of-mass energy of $\sqrt{s_{NN}} = 5.02$ TeV and $\sqrt{s_{NN}} = 8.16$ TeV are of the order of magnitude of 31–35 mbarn at the LHC. We compared our cross-section values with the values given in [1]. By doing these calculations for Pb–p collisions, we wish to give a contribution to the experiments that will be performed at the LHC. These calculations were done for the first time in [1] by using a simple scaling method. However, in our work, we used the Monte Carlo method described in detail above and we reached the confidential results as obtained in our previous works for different problems utilizing the same method. In this work, we did only the BFPP cross-section calculations of Pb–p collisions at the LHC. In future works, we are planning to do the EMD cross-section calculations of Pb–p collisions at the LHC and compare our results with the future expected experiment results.

REFERENCES

[1] M.A. Jebramcik, «Beam Dynamics of Proton–Nucleus Collisions in the Large Hadron Collider», Ph.D. Dissertation, 2020.

[2] ATLAS Collaboration, «Observation of a new particle in the search for the Standard Model Higgs boson with the ATLAS detector at the LHC», *Phys. Lett. B* **716**, 1 (2012).

[3] CMS Collaboration, «Observation of a new boson at a mass of 125 GeV with the CMS experiment at the LHC», *Phys. Lett. B* **716**, 30 (2012).

[4] R. Alemany *et al.*, «First proton–nucleus collisions in the LHC: the p–Pb pilot physics fill», Report CERN-ATS-Note-2012-094 MD, CERN, Switzerland (2012), https://cds.cern.ch/record/1496101

[5] M. Schaumann *et al.*, «Bound-free pair production from nuclear collisions and the steady-state quench limit of the main dipole magnets of the CERN Large Hadron Collider», *Phys. Rev. Accel. Beams* **23**, 121003 (2020), arXiv:2008.05312 [physics.acc-ph].

[6] J.M. Jowett *et al.*, «Proton–nucleus collisions in the LHC», in: «Proceedings of the 4$^{\rm th}$ International Particle Accelerator Conference (IPAC'13)», Shanghai, China 12–17 May 2013, p. 49, http://cds.cern.ch/record/1572994

[7] J.M. Jowett *et al.*, «The 2016 proton–nucleus run of the LHC», in: «Proceedings of the 8$^{\rm th}$ International Particle Accelerator Conference (IPAC'17)», paper No. TUPVA014, Copenhagen, Denmark 14–19 May, 2017.

[8] M.Y. Şengül, M.C. Güçlü, «Bound free electron–positron pair production accompanied by giant dipole resonances», *Phys. Rev. C* **83**, 014902 (2011).

[9] A. Aste, «Bound-free pair production cross-section in heavy-ion colliders from the equivalent photon approach», *Europhys. Lett.* **81**, 61001 (2008).

[10] A.N. Artemyev, V.G. Serbo, A. Surzhykov, «Double lepton pair production with electron capture in relativistic heavy-ion collisions», *Eur. Phys. J. C* **74**, 2829 (2014).

[11] R. Anholt, U. Becker, «Atomic collisions with relativistic heavy ions. IX. Ultrarelativistic collisions», *Phys. Rev. A* **36**, 4628 (1987).

[12] H. Meier *et al.*, «Bound-free electron positron pair production in relativistic heavy-ion collisions», *Phys. Rev. A* **63**, 032713 (2001).

[13] M.C. Güçlü, «Semi-analytic calculations for the impact parameter dependence of electromagnetic multi-lepton pair production», *Nucl. Phys. A* **668**, 149 (2000).

[14] M.Y. Şengül, «Bound-Free Pair Production Mechanism at the NICA Accelerator Complex», *Acta Phys. Pol. B* **52**, 1233 (2021).

[15] M.Y. Şengül, M.C. Güçlü, S. Fritzsche, «Bound-free electron–positron pair production in relativistic heavy-ion collisions», *Phys. Rev. A* **80**, 042711 (2009).

[16] M.Y. Şengül, «Bound-free electron–positron pair production mechanism at an electron-ion collider», *Int. J. Mod. Phys. E* **26**, 1750055 (2017).

[17] M.Y. Şengül, M.C. Güçlü, «Relativistic antihydrogen production by pair production with positron capture», *Prog. Part. Nucl. Phys.* **67**, 612 (2012).

[18] S.R. Klein, «Localized beampipe heating due to e^-capture and nuclear excitation in heavy ion colliders», *Nucl. Instrum. Methods Phys. Res. A* **459**, 51 (2001).

[19] S.R. Klein, «Heavy ion beam loss mechanisms at an electron-ion collider», *Phys. Rev. Spec. Top. Acc. Beams* **17**, 121003 (2014).